IBM DSD Report: Structure and Dynamics of Water in the Crystal of Myoglobin

IBM DSD

STRUCTURE AND DYNAMICS OF WATER IN THE MYOGLOBIN CRYSTAL

P. Procacci, G. Corongiu and E. Clementi

July 26, 1989 KGN-195

Kingston, New York

Copies may be requested from:
IBM, Department 48B, Building 963
Neighborhood Road
Kingston, New York 12401

Structure and Dynamics of Water in the Myoglobin Crystal

P. Procacci, G. Corongiu, and E. Clementi

IBM Corporation
Data System Division
Dept 48b / MS 428
Neighborhood Road
Kingston, New York 12401

Abstract

A molecular dynamics simulation of the hydrated myoglobin crystal is presented. The simulation model considers the unit cell filled with two rigid proteins and 856 mobile water molecules. Computed structure factors are in good agreement with observed scattering intensities. We found that a large percentage of water molecules have a translational mobility typical of a fluid system, consistent with the fact that only 40% of the simulated water molecules can be detected by x-ray crystallography. Computed solvent reorientational properties confirm the experimentally measured high dielectric relaxation rates. Protein segments characterized by large experimental B-values are found to be highly hydrated by water molecules with large mean square displacements.

Introduction

In recent years, due to the availability of supercomputers, simulations have become a powerful tool for studying the structure and dynamics of biological systems. Available theoretical works on the subject have focused the attention mainly on the structural and dynamical characterization of the macromolecules, often neglecting the role of water as a solvent.

Numerous protein simulations have been done *in vacuo*,[1-4] and systematically, too large mean square displacements (MSD) have been found. Such findings are even more discouraging if one considers that these studies can probe only fast vibration disorder, which is the only effective contribution to protein motions within the time generally spanned during simulations (i.e. 10-100 picoseconds). To the computed MSD one should add a static contribution arising from lattice disorder and a dynamical contribution due to the conformational motion of protein segments. Computer simulations do not account for lattice disorder, since the system is always assumed to be perfectly periodic under normal boundary conditions. Concerning the conformational diffusion, there are experimental evidences[5-9] that such kind of motions generally take place in a nanosecond time scale, a time which is not yet accessible to computer simulations.

It is seems now well established that the solvent role in protein simulations is essential.[7] In a recent molecular dynamics (MD) study of BPTI,[10] for example, the agreement between experimental and computed protein mobility was dramatically improved by including the solvent in the model. The main effect of the solvent, in MD simulations of hydrated proteins, with respect to the *in vacuo* case, is to slow down or even suppress collective motions of the side chains in the picosecond time domain. It is therefore reasonable to expect that keeping the protein rigid is a first order and straightforward approximation for investigating protein hydration at the structural level. Such approximation implies two assumptions: 1) In the picosecond time scale the protein is frozen in one particular conformational substate, and no direct coupling between water fast dynamic and slow protein conformational diffusion can take place. 2) The vibrational modes of the protein (stretching of bonds, bendings, torsions, etc.), although their time scale dynamics corresponds to that of the solvent, have amplitudes too small to modify substantially the potential hypersurface on which water molecules are constrained to move. At the dynamical level, the computed water properties can be affected, to some extent, by the rigid

protein approximation. However, in view of the two previous assumptions, we believe that the adopted model allows to extract valid general qualitative informations on the dynamical solvent behavior.

In the present study a Molecular Dynamics simulation of the water in the hydrated crystal of myoglobin is presented. Water structural and dynamical properties have been computed and compared, when available, with experimental data. A detailed analysis of the solvent hydration has been carried out and correlation between water connectivity at the protein surface and conformational diffusion of protein segment is discussed.

Model and computational procedure

Myoglobin crystallizes as a monoclinic lattice (space group $P2_1$) with two proteins per unit cell in general equivalent positions (x,y,z) and (-x,y+1/2,-z). The parameters of the unit cell are $A = 64.51$Å, $B = 30.91$Å, $C = 34.86$Å and $\beta = 105.8°$. The coordinates of the 1261 heavy atoms of the protein were provided by a recent X-ray refinement[11]. Hydrogen atoms were introduced according to geometric considerations yielding a total of 2532 atoms per protein.

The interaction between protein and water is represented by atom-atom potential functions obtained by a fit to *ab initio* computations done in our laboratory.[12-14] Each atom of the protein is assigned to a class; atomic number, partial electrostatic charge and chemical environment are criteria used to define a class[12]. The form of the interaction potential between one water molecule A and one protein P can be written as:

$$V_{A-P} = \sum_{i=1}^{3} \sum_{j=1}^{Natoms} \frac{q_i q_j C_{ij}^{ab}}{r_{ij}} + \frac{B_{ij}^{ab}}{r_{ij}^{12}} - \frac{A_{ij}^{ab}}{r_{ij}^{6}}$$

where index i runs over water atomic nuclei, j over protein atoms belonging to class a and b, respectively. Because no net charges were available for the haem group, an *ab initio* SCF computation was performed and partial electrostatic charges were determined by means of the Mulliken population analysis. Keeping in mind that the potentials are transferable for atoms belonging to the same class, we assigned each haem atom to a class according to the criteria previously summarized. Because of charged residues, we found on the myoglobin protein a net charge of +2, which under experimental conditions is

neutralized by counterions. To simplify the work, instead of including counterions, we neutralized the negative charge excess by distributing -2 electrons among all myoglobin atoms; in this way each partial charge was diminished by 0.0008 electrons. The water-water interaction was described by the MCY potential;[15] 856 water molecules were introduced in the unit cell yielding a crystal density of 1.2705 g/cm^3. The starting configuration was obtained from the last configuration of a previous Monte Carlo simulation[16].

The integration of Newton-Euler equations was carried out in the N,V,E ensemble adopting a fifth order Gear algorithm for the translational motions. For the rotational motions we used a sixth order integrator for the quaternions, combined with a second order quaternion scheme for recasting at each time step the angular velocities.[17] Long range effects due to electrostatic interaction were corrected with the Ewald sum procedure.[18] In the present case, since we are dealing with a lattice where also the solvent connectivity shows an high level of periodicity (about 40% of the water molecules in the unit cell can be detected by x-ray crystallography[11]), we may confidently expect the perfect lattice approximation to be fairly reliable and physically convincing. Moreover, a long range correction which allows a suppression of the energy pumping mechanism induced by the potential truncation[19] is especially required in the present case: When a cut-off at 15Å is adopted, the total energy drift observed during the simulation is of the order of $1.6 KJ \times mole^{-1}$ per picosecond (see Fig. 1a). Inclusion of long range interaction by means of the Ewald procedure yields full conservation of the total energy (see Fig. 1b). The simulation run was carried on for about 50 ps, with a time step of 0.5 fs. The first 20 ps were considered as system equilibration, and the remaining 30 ps were used for statistical analysis, dumping particle coordinates and velocities every 10 steps, corresponding to a Δt of 5 fs. With this choice of the integration time step, during the last 30 ps the total energy was conserved with a maximum fluctuation of 0.004 KJ/mole per ps and the velocities were never rescaled. The average temperature and average potential energy were 304.4 +/- 8.15 K and -73.0989 +/- 0.1333 $KJ\ mole^{-1}$, respectively.

General properties of the solvent

Although the structure and dynamic of myoglobin has been widely studied in an enormous amount of experimental works (see ref. 18 for a review), only a few experimental data are available on the hydration pattern both in crystal and in solution. In a X-ray study by Takano[21] 82 water molecules per protein were individually determined. Phillis[22] and Parak[11], in two distinct X-ray refinements on deoxy and met-myoglobin, found about 160 water molecules per protein, many of them having high liquidity factors and low occupancies. In none of these studies, however, the inferred model for the solvent yielded a completely satisfactory agreement with the observed scattering intensities.

The static structure factors can be computed from the simulation data using the following equation

$$F(\mathbf{k}) = \sum_{j=1}^{NATOMS} f_{jT}(|\mathbf{k}|) \exp(i\mathbf{k} \cdot \mathbf{r}_j) + \frac{1}{nt} \sum_{i=1}^{nt} \sum_{j=1}^{NSOLV} f_j(|\mathbf{k}|) \exp(i\mathbf{k} \cdot \mathbf{r}_{ij})$$

The first term on the right side of this equation is the contribution of the protein atoms to the overall scattered radiation. The temperature form factors f_{jT} have been computed from tabulated atomic form factors f_j and Debey-Waller factors B obtained from X-ray studies[11], according to the relation

$$f_{jT} = f_j \exp[-B(\sin\theta/\lambda)^2]$$

with

$$2\sin\theta/\lambda = |\mathbf{k}| \quad ; \quad B = 8\pi^2 < x^2 >$$

In the above relations θ and λ are, respectively, the scattering angle and wavelength of the incident beam, $\mathbf{k}$ is a vector of the reciprocal lattice and $< x^2 >$ is the experimental MSD. The second term, computed from the simulation data, represents the contribution to the structure factors due to the solvent: nt is the number of time averages considered within the 30 ps time span. In Fig. 2 computed (dashed line) and experimental[21] (solid line) X-ray scattering intensities are compared; the structure amplitude, in electrons, is plotted as a function of $\sin(\theta/\lambda)^2$. In order to assess the water contribution to the overall scattering intensities we also reported in the same figure (dotted line) the amplitudes obtained when only the protein atoms are considered (*i.e.* the contribution due to the first term of

the equation.) It is evident that the role of the solvent is essential in determining the shape of intensity radial distribution for low resolution. Inclusion of the solvent gives rise to the first peak at $(\sin\theta/\lambda)^2 = 0.005$, also present in the experimental curve, and shifts in the correct direction the second peak at around $(\sin\theta/\lambda)^2 = 0.01$. It should be noted that, in our model, the contribution of the rigid protein framework accounts for the dumping due to all kinds of displacements through the experimental Debye-Waller factors, whereas the solvent contribution probes the water structure and liquidity resulting from a picosecond time scale simulation. The satisfactory agreement with the X-ray measurements appears to sustain the assumption that the protein motions do not affect significantly the solvent structure.

In Fig. 3, radial distribution functions (RDF) and relative coordination numbers versus distance are reported and compared with those obtained in an earlier calculation for bulk water at 298 K[21]. The curve marked with the legend 'o(w)-o(w)' refers to oxygen-oxygen water RDF in the myoglobin crystal; the curve 'o(w)-o(w) + p' has been computed by including also the protein heavy atoms. The curve and 'o(w) - p', which represents the radial distribution of protein heavy atoms with respect to a solvent molecule, can be analytically obtained by weighted difference of the two previous RDFs.

In the solvent-solvent RDF (o(w)-o(w)), the position of the first peak, corresponding to the first solvation shell, shows no significant differences when compared to the bulk case. The enhancement of the intensity, with respect to bulk, and probably also the weak maxima at 4.9 and 5.6 Å, are an artifact of the computation because of unhomogeneity of the water density in the unit cell. In the 'o(w) - o(w) + p' and 'o(w) + p' curves, the first peak is clearly shifted toward shorter distances which is an indication of strong interaction between solvent and protein surface.

In Fig. 3b, coordination numbers, obtained by integrating the corresponding RDF's, are reported. Bulk water shows a well defined coordination number of five at about 3.5Å. For the 'o(w)-o(w) + p' curve it is hard to determine unambiguously a first shell coordination number, since the behavior is almost linear between 2.9 and 3.5 Å. However, pentacoordination is reached at 3.28 Å; at this distance the average repartition of the five coordination sites of a solvent molecule is found to be 2.8 water molecules (o(w) - o(w)) and 2.2 protein atoms (o(w) - P). The heavy coordination of water molecules by protein atoms at short distances suggests that the solvent is packed at the protein surface.

The solvent dynamical behavior can be investigated by computing time dependent correlation functions of the form

$$C(h) = \frac{< f(h+t)f(t) >}{< f(t)f(t) >}$$

where the brackets indicate averages over molecules and time origins. The center of mass velocity autocorrelation function (VAF) provides information about the diffusional regime, and its power spectrum is related to the density of the states of the translational modes in the far infrared region. In Fig. 4a, VAF for water in the myoglobin crystal is compared to that computed for bulk water at the same temperature[24]. The average time for sign reverse, in the myoglobin water (dotted line) is about 20 fs faster with respect to bulk (solid line), and the curve lies for a longer time below zero, suggesting that diffusional motions are strongly hindered. This behavior for the VAF was expected, since around 40% of the solvent molecules in the unit cell are visible in X-ray electron density maps[11,22] and therefore do not diffuse. Comparison of the power spectra of the VAFs is provided in Fig. 4b. The density of the states for bulk water shows a sharp peak at around 50 cm^{-1} and a second one at 200 cm^{-1}. For the myoglobin water the first peak is slightly shifted toward higher frequencies and the associated band is broadened, and at 200 cm^{-1} only a shoulder can be observed. Some modes appear in the region between 300 and 450 cm^{-1} probably due to vibrations of solvent molecules tightly bound at the protein surface (see next section) rather than to ice-like behavior[25]. The time integral of the VAF gives the diffusion coefficient. The computed value is 0.13×10^{-5}, to be compared to 2.60×10^{-5} in bulk water.[26]

The translational diffusional regime can also be investigated by monitoring the mean square displacements computed according to

$$< x^2(h) > = < |\mathbf{R}(t+h) - \mathbf{R}(t)|^2 >$$

For liquids, the mean square displacement is a linear function of time and the limiting value of the slope, for t tending to infinity, is equal to 6D where D is the self-diffusion coefficient. The mean square displacement plotted versus time (Fig. 5), shows definitely a liquid-like behavior. As extensively discussed in the next section, the almost linear trend of RMS's is determined by a rather large percentage of solvent molecules able to retain, even in the crystal, a high level of translational mobility.

Reorientational properties for water in a crystal of met-myoglobin have been recently investigated by dielectric relaxation measurements.[8] Although a direct comparison of collective properties[32] to dielectric relaxation rates is beyond the possibility of the present study (because of the short simulation), qualitative indications about rotational diffusion can be obtained by computing the single particle dipolar autocorrelation function according to

$$C_l(h) = < P_l(\mathbf{e}(t+h) \cdot \mathbf{e}(t)) >$$

where P_l is the *l-th* Legendre polynomial and **e** is a unit vector in the direction of the water dipole. The integral of $C_1(t)$ from 0 to infinity, assuming a Debye exponential decay for $t > 30$ ps, yields a value of 88 ps for the average dipolar reorientation time, which is about 20 times larger than the computed value for bulk water.[27] The limited rotational diffusion of the dipolar axis, as found from the simulation, qualitatively agrees with the large dielectric relaxation time (of the order of 100 ps) experimentally determined.

Local structural and dynamical properties

Computation of significant local structural and dynamical properties is not straightforward since it is difficult to define sub-ensembles for which one can compute meaningful statistical averages. Our first approach was not dissimilar from the one adopted in a simulation of solvated BPTI.[10] We partitioned the water molecules among four classes. Those molecules which remain, during the whole simulation length, within a 3.5 Å shell from some heavy atoms of charged, polar and neutral residues, are defined to be members of class I, II and III, respectively; members can be shared within these classes. In class IV are gathered all the remaining molecules, namely those which either are most of the time more than 3.5 Å away from any residue, or are exchanging among the three different classes defined above; members of class IV cannot be simultaneously members of any other class.

In Table I, some general properties of each class are reported. As expected, although the hydrophobic residues are the most numerous, the highest level of solvation is found for charged and polar residues and, correspondingly, water-protein interaction energies are stronger for hydrophilic groups. Water molecules in class IV constitute about 40 % of the

total and are characterized by weaker interactions with the protein. Water molecules in classes I, II and III have small MSDs, and appear to remain for long time at the protein surface, as it can be seen from the typically solid-like behavior of the MSD time dependency reported in Fig. 6. The MSDs, here reported, are somewhat smaller than those experimentally determined for the bound water molecules.[11] We believe that this discrepancy can be ascribed to the shortcomings of the simulation model: since the protein is kept rigid, the water mobility at myoglobin surface is probably reduced by the lack of coupling between solvent and side chain's vibrational modes.

Water molecules in class IV show a completely different diffusional regime, typical of a liquid system. The corresponding MSD time dependence (see Fig. 6) is almost linear and the self-diffusion coefficient obtained from the limiting slope of the straight line is about one third of that of pure water at the same temperature. A similar behavior is expected to occur in solution, where the distances between water and protein atoms can be very large. In the case of the myoglobin crystal, at least 2/3 of the volume of the unit cell[28] is occupied by the two proteins and the largest distances of any solvent molecules from the protein surface can never exceed 6.0Å. Nevertheless, it appears that nearly all the water molecules not belonging to the first solvation shell of some residues, despite their nonnegligible interaction energy with the protein (-4.2 Kcal/mole), are able to retain a high level of translational disorder.

The average time of solvent exchange between the protein first hydration shell and the mobile layer (e.g. members of class IV) can be monitored by computing, for charged, polar and neutral residues, the time dependent correlation function

$$n(t) = \frac{1}{nt} \sum_{j}' \sum_{i=1}^{nt} Q_j(t_i, t)$$

where $Q_j(t_i, t)$ is a property of molecule j: It assumes the value 1 if the molecule remains within the defined solvation shell (e.g. 3.5Å) during the time interval $t_i \leq t \leq t_i + t$, and 0 otherwise. The inner sum denotes time averages over the whole simulation length. For the correlation time $t = 0$, $n(t)$ is simply the average coordination number of the solvated residues; at short times the function decays exponentially and the residence time in the solvation shell is given by the exponential decay time[29]. Plots of these functions for charged, polar and neutral residues are shown in Fig. 7. The curves have been normalized

by the corresponding factor $n(0)$ to achieve direct comparison. As it can be observed from the figure, the residence time increases with the residue's hydrophilicity.

Further informations about dynamical behavior of the solvent can be gathered by computing local time dependent correlation functions. In Fig. 8 the power spectra of the velocity autocorrelation function are plotted for each class. It is evident that the peak at 50 cm^{-1} in the spectrum of Fig. 4b is predominantly determined by the translational motion of the mobile water molecules in class IV, whose density of the states is nearly indistinguishable from that of bulk water. The spectra of water molecules in classes I, II, and III have broader peaks, shifted towards high frequencies (between 100 and 200 cm^{-1}). For molecules in class I a second peak appears at 350 cm^{-1}, probably due to vibrational modes of solvent at the charged amino groups af Arg and Lys, and at the carboxy groups of Glu and Asp, where electrostatic interactions are very strong.

Experimental work, particularly by Parak's group,[5-9] suggests that protein conformational motions are probably strongly correlated with the structure and the dynamics of the surrounding solvent. It has been inferred[7] that the fluctuations of the electric field produced by the hydration water at specific places of the protein surface might induce sudden annihilations of the potential barrier between two local conformations, such that a transition between *conformational substates*[9] can be triggered. As suggested by Moessbauer absorption measurements, the frequency of these events in myoglobin appears to be in the nanoseconds time domain.[8,9] If this mechanism is correct, it should be possible to detect whether the *local* structural arrangement and the dynamics of the solvent, in the picosecond time scale, is related somehow to the mobility of the protein environment obtained from experimental B-values.

In order to reveal possible correlations, the experimentally determined B-values of the protein atoms have been used for defining new solvent classes. Water molecules within a 3.5Å distance from protein atoms having B-values in the range 0-10, 10-15, 15-20, 20- $Å^2$, belong to classes, A, B, C, and D, respectively. Again, water molecules can be shared among classes. Those molecules more than 3.5 Å away from any protein atom are, obviously, members of the class IV defined previously. In Table II the resulting properties are summarized. It can be observed that the number of water molecules and the water - protein stabilization energy increase steadily from class A to class D, namely with increasing B-values of the solvated residues. In addition, in general particularly rigid seg-

ments are buried inside the proteins.[5] However, in the myoglobin case most of the helices and loops show a certain degree of exposure (see Fig. 9) and, therefore, it is difficult to define a clear solvent-protein interface. It should be stressed that, from the data in Table II, a) the residues which are embedded in regions of low conformational disorder are also poorly solvated; b) regions of the protein with high conformational disorder seem to be located in correspondence of local minima of the water - protein potential hypersurface; 3) the computed MSDs are generally larger for water molecules solvating mobile segments.

Fine details of hydration patterns can be revealed by computing residue - water oxygen RDFs. Such properties are of particular interest, since only incomplete experimental data are available for solvent arrangements around myoglobin. The solvent - residue radial distribution functions, averaged over the two proteins in the unit cell, are presented in the diagram of Fig. 10 for each residue (x-axis) at selected distances. It can be noticed that most of the peaks fall in the range enclosed between 2.6 and 2.8 Å, which roughly corresponds to the distance from the oxygen atom of one water molecule hydrogen bonded to a protein atom. The sharpest peaks generally correspond to polar and charged residues, whereas gaps are mainly found for neutral residues. There are exception to this trend especially on hydrophobic groups where often a high level of hydration is found. Fig. 11 shows the coordination number at 3.5 Å versus residue number. High level of solvation on hydrophobic groups can be detected for example at the Val-1, Trp-7, Val-13, Phe-43, Leu-49 and Pro-120. Local computed MSDs for the solvent hydrating neutral groups (see Table I) show that, although hydrophobic residues are in general less hydrated than charged and polar side chains, those who happen to be solvated are often surrounded by water molecules arranged in stable and ordered configurations.

Conclusions

An accurate structural characterization of the solvent in the crystal of myoglobin, obtained from the analysis of molecular dynamics simulations, has been presented. Computed and measured X-ray scattering intensities have been compared and our overall solvent structure was found to agree quite well with the experimental results. The hydration pattern on the myoglobin crystal appeared to be reasonable[30] and coherent with that obtained in analogous simulation where the time span was longer and the model included the relaxation of protein internal degrees of freedom.[10,31] The computed

translational and reorientational properties of the solvent are consistent with available experimental data.

As suggested in Ref. 8, we gathered strong indication that a correlation may exist between water connectivity and protein dynamics. On the other hand, we also believe that at the dynamical level, some of the computed properties are probably affected by the fixed protein approximation of this study.

Determination of the solvent local dynamical properties, at the residue level, would complete the picture of the role played by the solvent in protein dynamics. However, this task might require inclusion of the low frequency internal modes of the protein, namely those which can couple with water librations and translations.

However, it should be recalled that the assumption on which we based our original model still remains valid. If the simulation time spans not more than some tenths or even some hundreds of picoseconds, then in such a time scale, the proteins are generally not able to undergo major collective motions and, therefore, the computed protein atoms MSDs must be lower or at most equal to those determined by X-ray. Further, additional indirect informations about protein conformational diffusion can be gathered possibly by investigating the dynamical behavior of the solvent with a more accurate model. In particular, local dipolar autocorrelation functions and residence times can be computed and eventually correlated to protein dynamics, to probe the fluctuations of the electric field at specific regions of the protein surface. Work is in progress in these directions.

Acknowledgment

We acknowledge Prof. F. Parak for many interesting and extensive discussions held during his visit to our laboratory and for providing us his experimental data prior to publication. We also wish to thank Drs. M. Marchi and U. Niesar for discussions and suggestions.

References

1. J.A. Mc Cammon, B.R Gelin and M. Karplus, Nature (London), **267**, 585 (1977)
2. M. Karplus and J.A. McCammon, CRC Crit. Rev. Biochem., **9** , 293 (1981)
3. M. Levitt, J. Mol. Biol., **168**, 595 (1983)
4. R. Elber and M. Karplus, Science, **235**, 318 (1987)
5. F. Parak and H. Formanek, Acta Crystallogr. **27A** , 573 (1971)
6. H. Frauenfelder, G. Petsko and D. Tsernoglu, Nature **280** , 558 (1979)
7. G.P. Singh, F. Parak, S. Hunklinger and K. Dransfeld, Phys. Rev. Letters, **47**, 685 (1981)
8. F. Parak, E.W. Knapp and D. Kucheida, J. Mol. Biol., **161**, 177 (1982)
9. H. Frauenfelder, F. Parak and R.D. Young, Ann. Rev. Biophys. Chem., **17**, 451 (1988)
10. M. Levitt and R. Sharon, Proc. Natl. Acad. Sci. USA, **85** , 7557 (1988)
11. F. Parak, private communication.
12. E. Clementi, F. Cavallone and R. Scordamaglia, J. Am. Chem. Soc., **99**, 5531 (1977)
13. G. Ranghino and E. Clementi, Gazz. Chem. Ital., **108**, 157 (1978)
14. G. Ranghino, E. Clementi and S. Romano, Biopolymers, **22**, 1449 (1983)
15. O.E. Matsuoka, E. Clementi and M.J. Yoshimine, J.Chem.Phys., **64**, 1351 (1976)
16. G. Corongiu, P. Procacci, E. Clementi and F. Parak, (to be published).
17. R. Sonnescheim, J. Comp. Phys., **59**, 347 (1985)
18. S. W. De Leeuw, J. W. Perram and E. R. Smith, Proc. R. Soc. Lond., A **373**, 27 (1980)
19. D. J. Tildesley in *Molecular liquids - Dynamics and Interactions*, A. J. Barnes et al. (Eds.), 519-560 (1984)
20. W. Bialek and R. F. Goldstein, Biophys. J., **48**, 1027 (1985)
21. T. Takano, J. Mol. Biol., **110**, 537 (1977)
22. S. E. V. Phillips, J. Mol. Biol., **142**, 531 (1980)
23. K. S. Kim and E. Clementi, J. Am. Chem. Soc., **107**, 5504 (1985)
24. G. C. Lie and E. Clementi, Phys. Rev. A, **33**, 2679 (1985)
25. M. Marchi, J.S. Tse and M. Klein, J. Chem. Phys., **85**, 2414 (1986)
26. K. Krynicki, C. D. Green and D. W. Sawyer, Discuss. Faraday Soc., **66**, 199 (1978)
27. M. Wojcik and E. Clementi, J. Chem. Phys., **85**, 3544 (1986
28. B. Schoenborn, J. Mol. Biol., **201**, 741 (1988)

29. P. A. Madden and R. V. W. Impey, *Computer simulation of chemical and biomolecular systems*, D. L. Beveridge and W. L. Jorgensen, Eds., The New York Academy of Sciences, New York (1986)
30. N. Thanni, N. Thorzon and J. R. Goodfellow, J. Mol. Biol., **202**, 637 (1988)
31. H. J. C. Berendsen, V. F. van Gunsteren, H. R. J. Zwenderman and R. G. Geurtsen, *Computer simulation of chemical and biomolecular systems*, D. L. Beveridge and W. L. Jorgensen, Eds., The New York Academy of Sciences, New York (1986)
32. G. I. Szasz and K. Heinzinger, J.Chem. Phys., **79**, 3467 (1983)

Figure captions

Figure 1. Trends of kinetic and total energy as a function of time without (top) and with (bottom) the Ewald sums.

Figure 2. Computed (dashed line) and experimental (solid line) radial structure amplitudes distributions $|F(\mathbf{k})|$. The dotted line represents the contribution to $|F(\mathbf{k})|$ from the protein atoms.

Figure 3. Radial distribution functions (left) and corresponding coordination numbers (right). Dot-dashed line: oxygen - oxygen in bulk water; dashed line: oxygen oxygen in the myoglobin crystal; solid line: oxygen - oxygen + heavy atoms; dotted line: oxygen - heavy atoms.

Figure 4. Translational velocity autocorrelation functions (left) and corresponding spectra (right) for water in bulk (dashed line) and in the myoglobin crystal (solid line). In inset b) each of the two spectra has been normalized to the corresponding highest peak.

Figure 5. Water mean square displacements as a function of time.

Figure 6. Mean square displacements of water molecules belonging to classes I (solid line), II (dashed line), III (dotted line) and IV (dot-dashed line).

Figure 7. Time dependent coordination numbers for charged, polar, and neutral residues.

Figure 8. Power spectra of the VAFs for water molecules in classes I (solid line), II (dashed line), III (dotted line), and IV (dot-dashed line). The curves have been normalized to the highest value of the class IV spectrum.

Figure 9. 3-D representation of myoglobin. Dark grey segments corresponds to charged, light grey to polar and shiny grey to neutral residues. The haem is represented by a *ball and stick* model.

Figure 10. Radial distribution functions versus residue number at selected distances.

Figure 11. Coordination number at 3.5Å as a function of residue number. Full squares correspond to charged, crosses to polar, and empty squares to neutral residues.

Table I. Properties of the water at charged, polar and neutral residues.

property	class I	class II	class III	class IV
Residue type	charged	polar	neutral	
Number of residues	44	32	77	-
Number of water molecules	385	138	150	337
MSD ($Å^2$) after 15 ps	0.40	0.37	0.31	4.24
Water-protein energy (KJ/mole)	-97.8	-65.8	-30.7	-17.7

Table II. Properties of the water in classes A, B, C, and D.

property	class A	class B	class C	class D
B-value range	0-10	10-15	15-20	20-
Number of heavy atoms	956	918	414	232
Number of water molecules	101	205	238	178
MSD (Å^2) after 15 ps	0.20	0.34	0.39	0.38
Water-protein energy (kJ/mole)	-34.8	-74.8	-93.7	-104.8

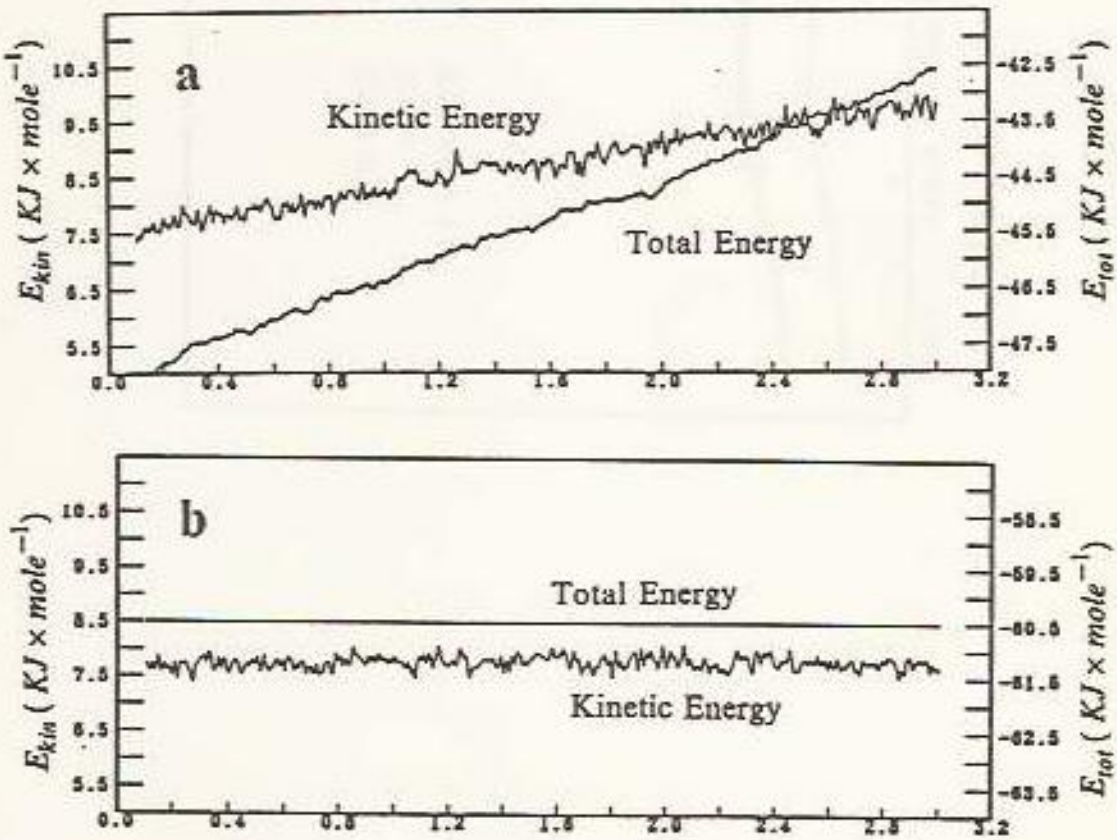
a
Kinetic Energy
Total Energy
E_{kin} ($KJ \times mole^{-1}$)
E_{tot} ($KJ \times mole^{-1}$)
10.5
9.5
8.5
7.5
6.5
5.5
-42.5
-43.5
-44.5
-45.5
-46.5
-47.5
0.0
0.4
0.8
1.2
1.6
2.0
2.4
2.8
3.2
b
Total Energy
Kinetic Energy
E_{kin} ($KJ \times mole^{-1}$)
E_{tot} ($KJ \times mole^{-1}$)
10.5
9.5
8.5
7.5
6.5
5.5
-58.5
-59.5
-60.5
-61.5
-62.5
-63.5
0.0
0.4
0.8
1.2
1.6
2.0
2.4
2.8
3.2

Fig. 1

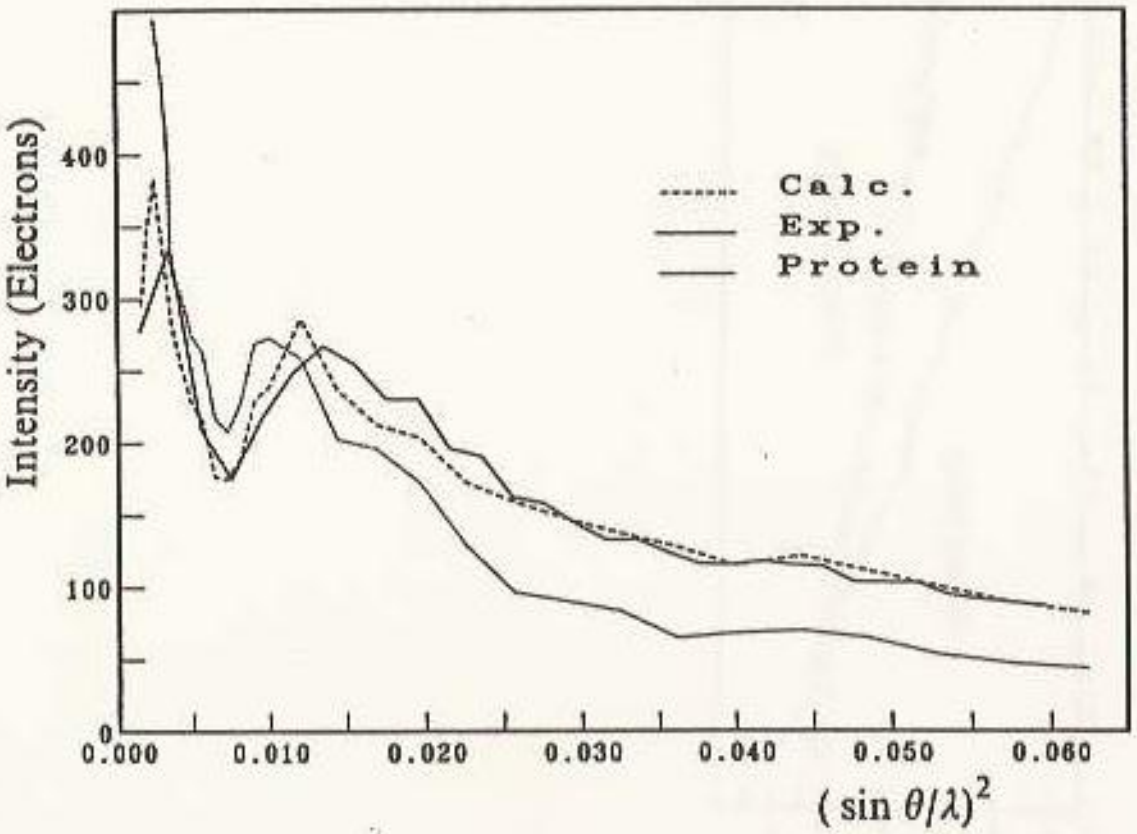
Intensity (Electrons)
400
300
200
100
0
0.000
0.010
0.020
0.030
0.040
0.050
0.060
(sin θ/λ)²
Calc.
Exp.
Protein

Fig. 2

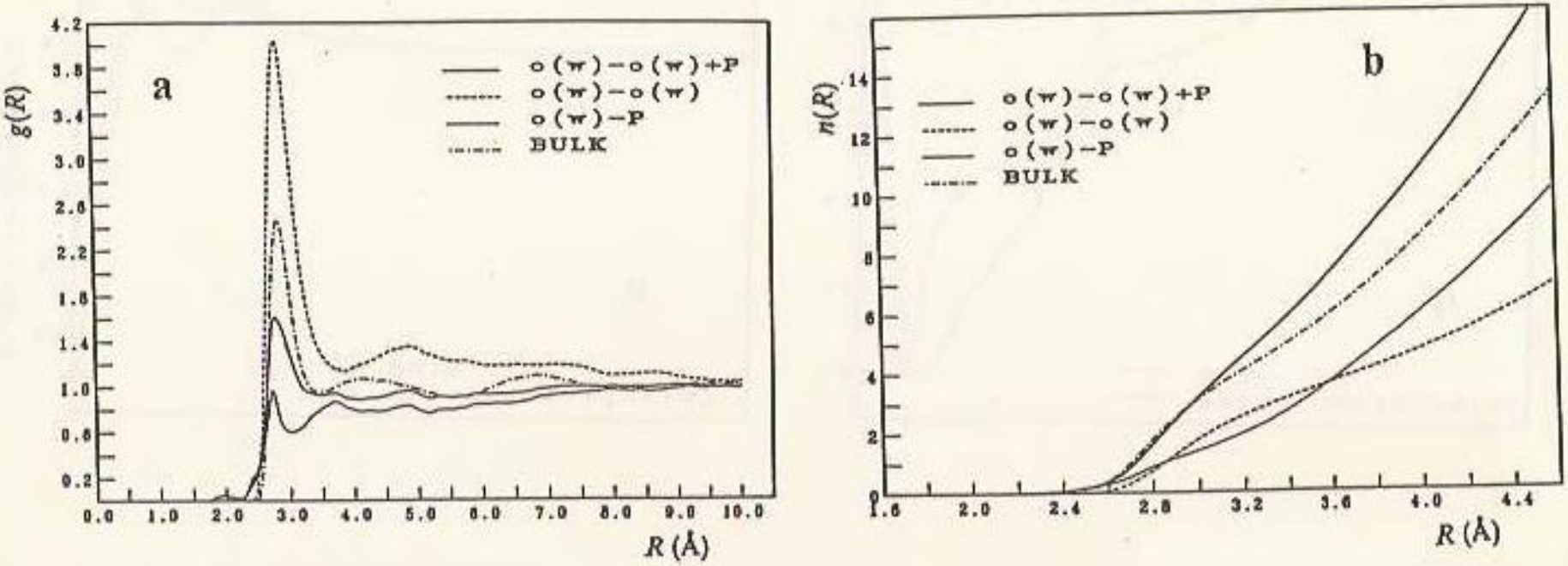

Fig. 3

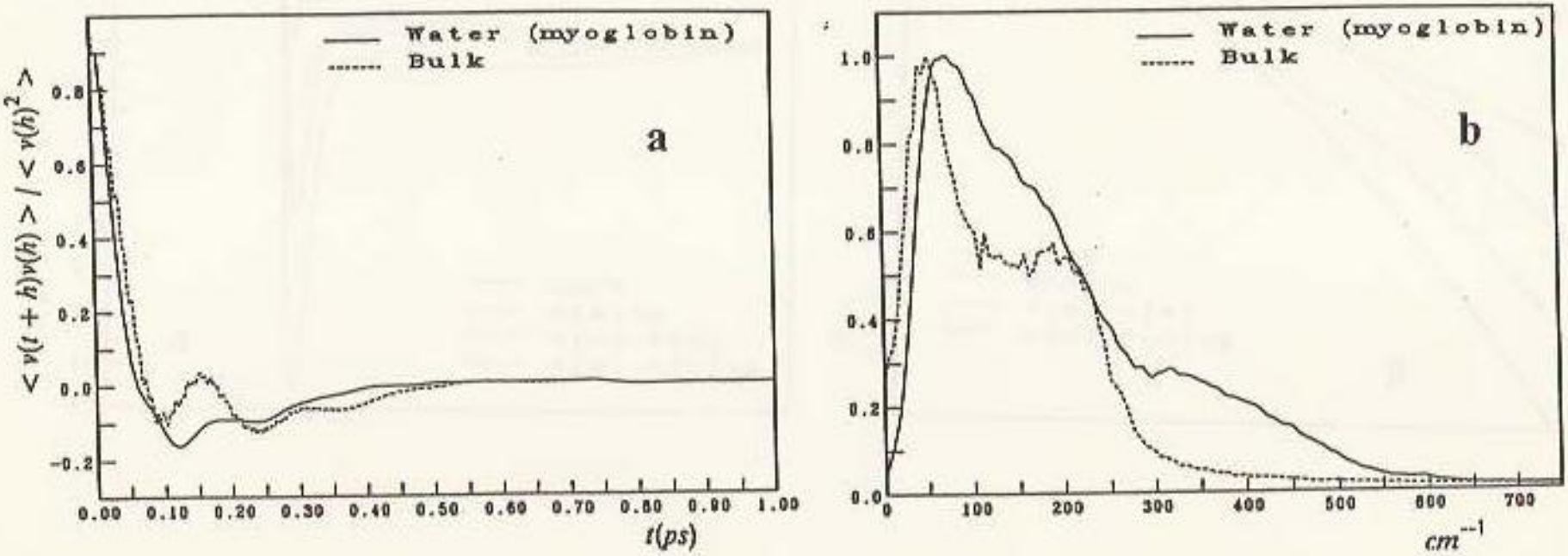
Water (myoglobin)
Bulk
a
$< v(t+h)v(h) > / < v(h)^2 >$
t(ps)
Water (myoglobin)
Bulk
b
cm^{-1}

Fig. 4

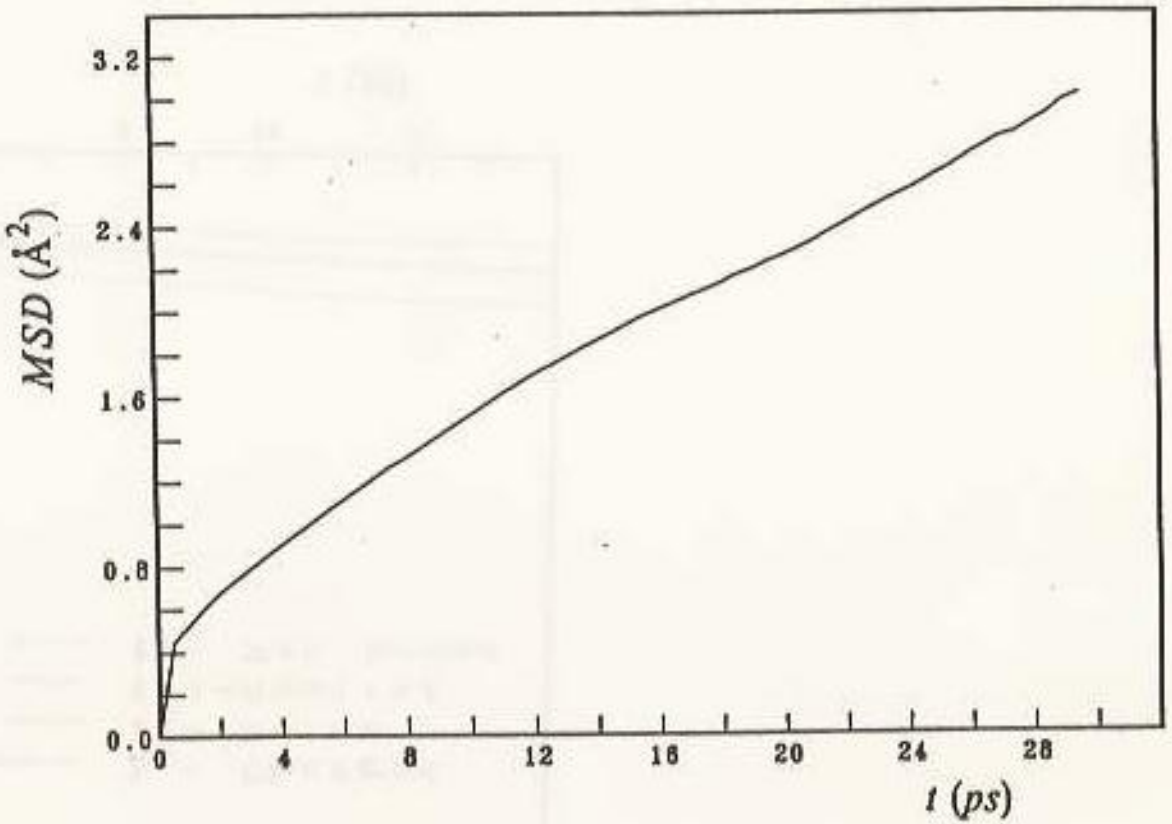

Fig. 5

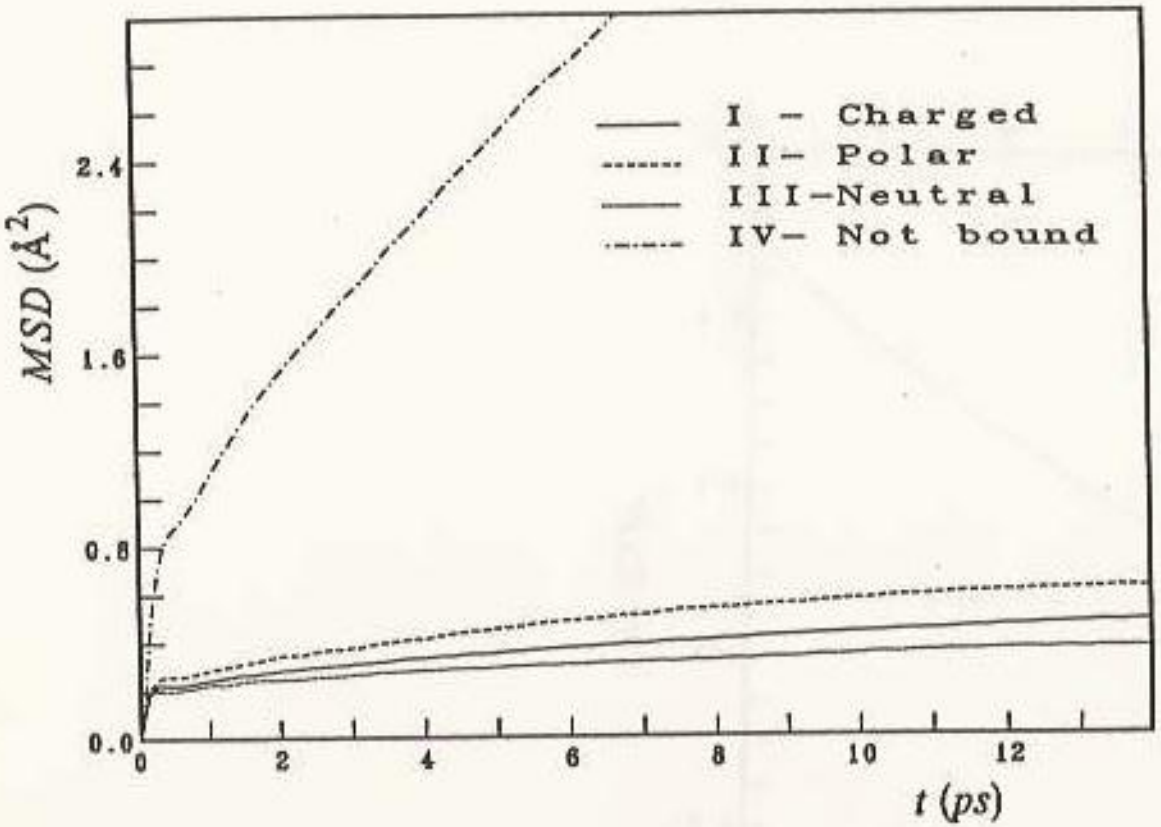
I - Charged
II- Polar
III-Neutral
IV- Not bound
MSD (Å²)
2.4
1.6
0.8
0.0
0
2
4
6
8
10
12
t (ps)

Fig. 6

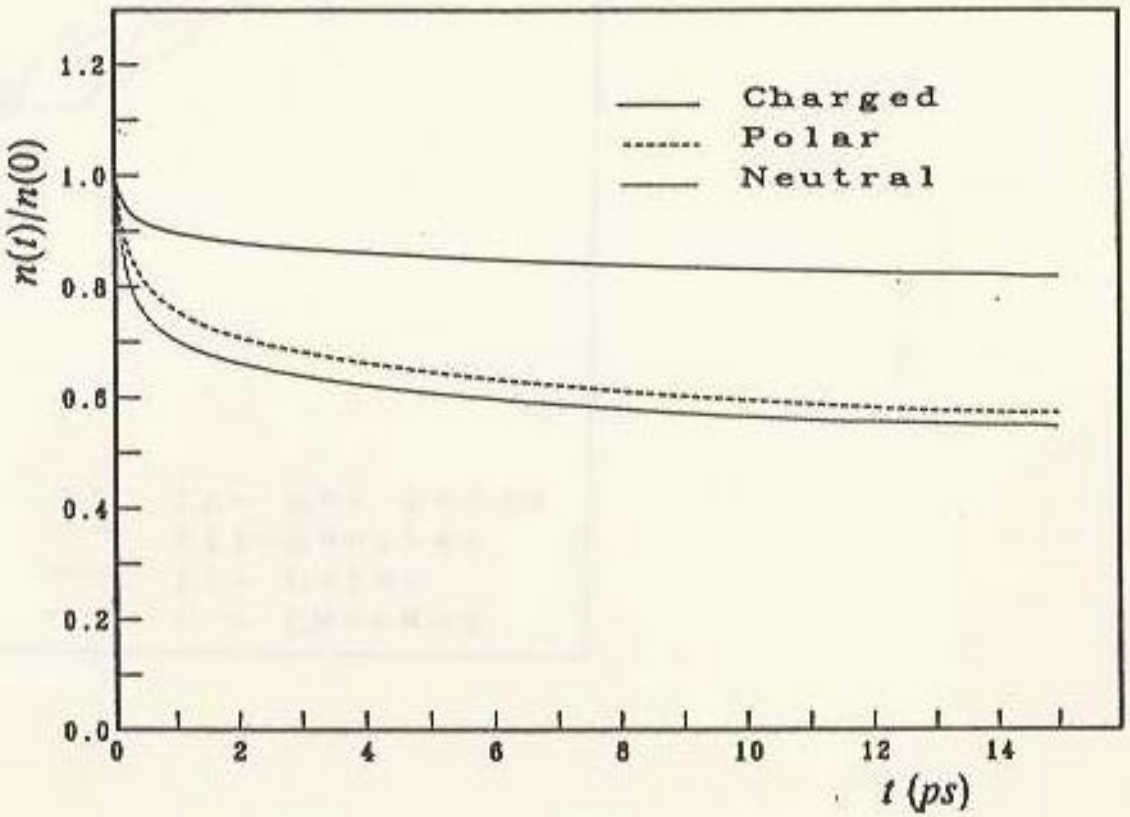
Charged
Polar
Neutral
n(t)/n(0)
1.2
1.0
0.8
0.6
0.4
0.2
0.0
0
2
4
6
8
10
12
14
t (ps)

Fig. 7

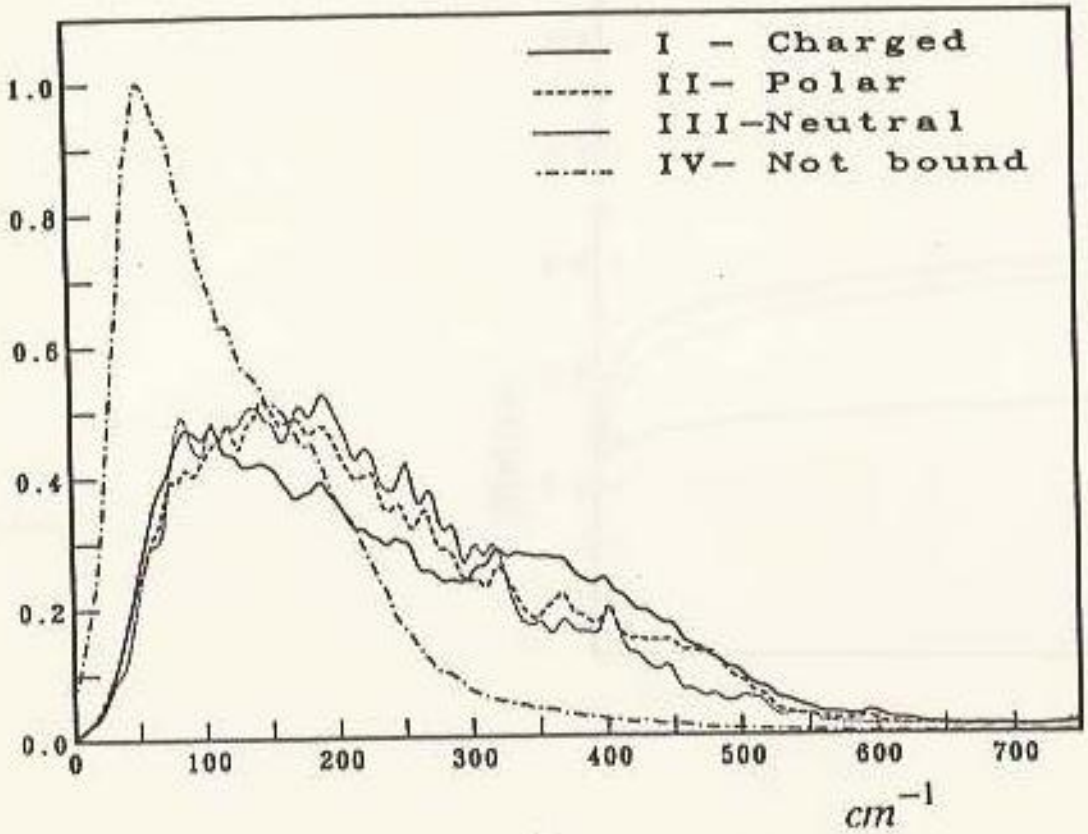
I - Charged
II- Polar
III-Neutral
IV- Not bound
1.0
0.8
0.6
0.4
0.2
0.0
0
100
200
300
400
500
600
700
cm^{-1}

Fig. 8

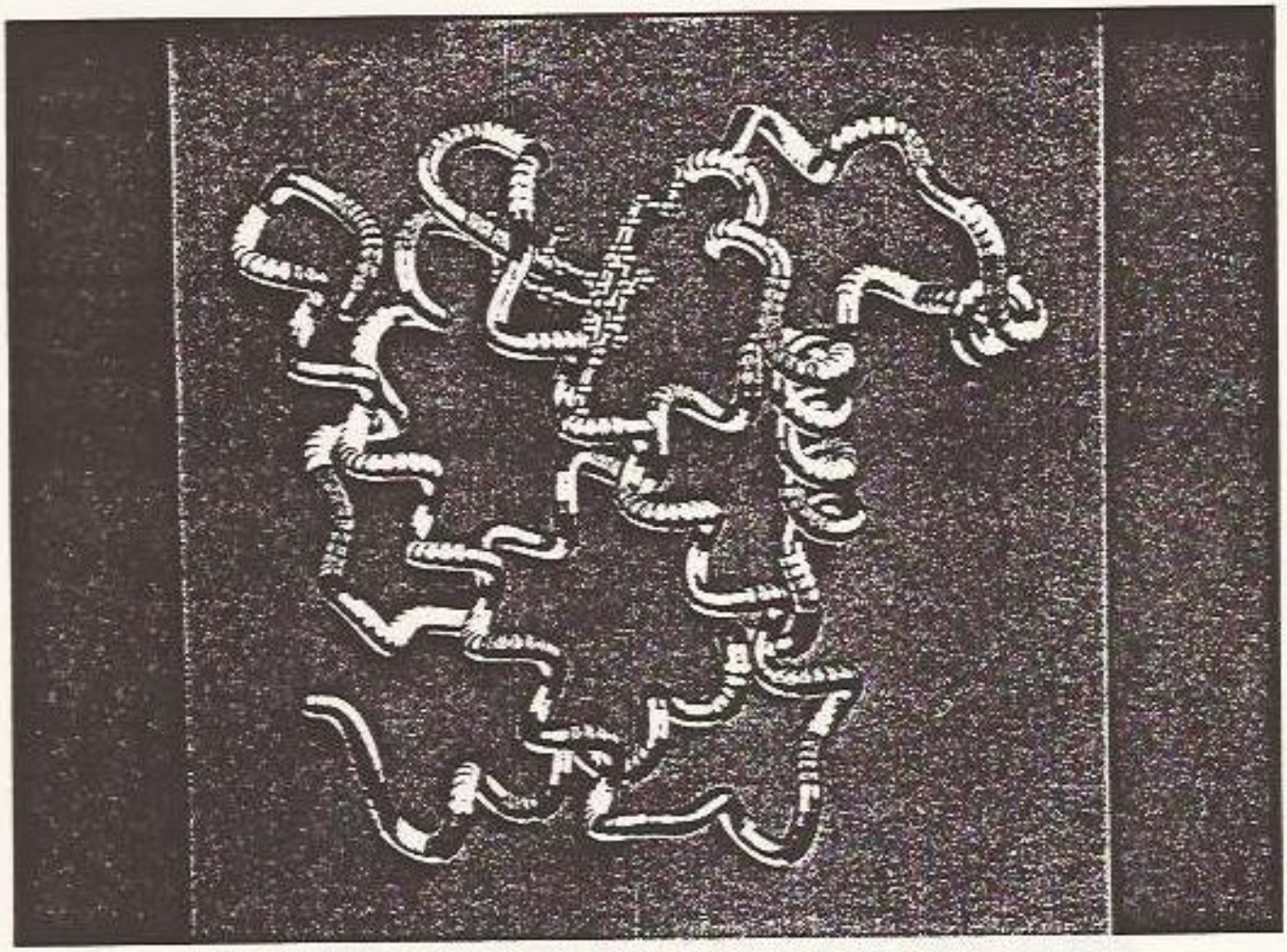

Fig. 9

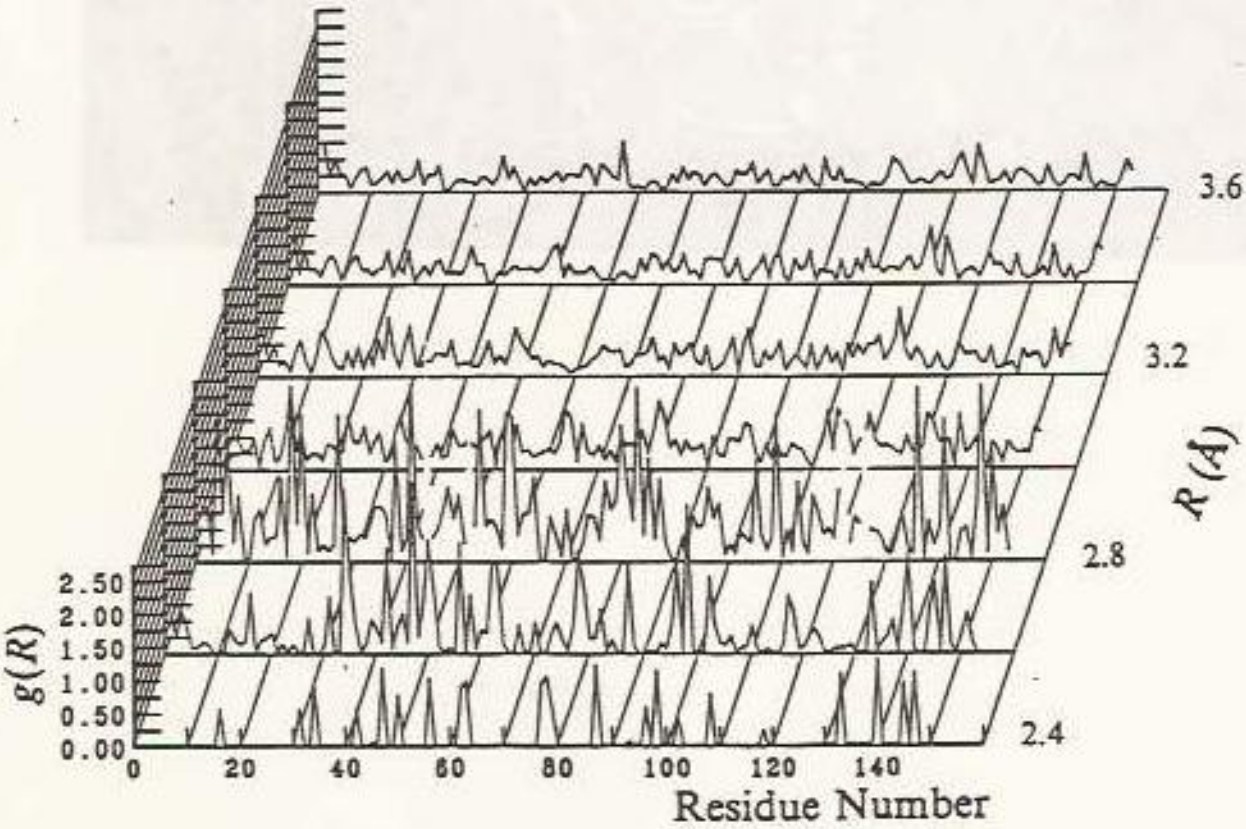
g(R)
2.50
2.00
1.50
1.00
0.50
0.00
0
20
40
60
80
100
120
140
Residue Number
2.4
2.8
3.2
3.6
R (Å)

Fig. 10

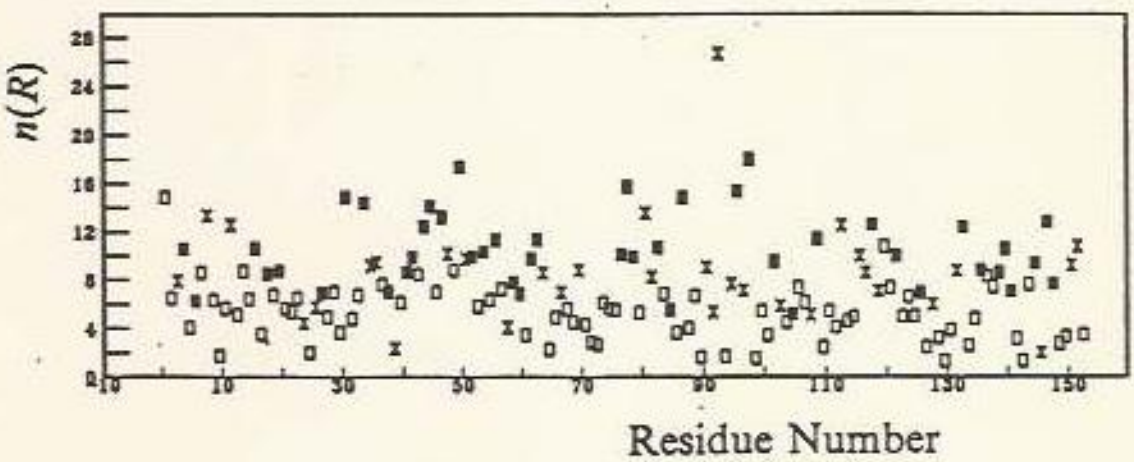

Fig. 11